8th International Congress on the Science and Technology of Steelmaking
2–4 August 2022, Montreal, Que., Canada
DOI 10.33313/531/036

# Numerical Study on the Mixing Characteristics in the Argon Oxygen Decarburization Process

Zhongfu Cheng[1], Yannan Wang[2], Abhishek Dutta[3], Bart Blanpain[1], Muxing Guo[1], Annelies Malfliet[1]

[1]Department of Materials Engineering, KU Leuven
Kasteelpark Arenberg 44, Leuven, Belgium, 3001
Phone: +32 16372344
Email: zhongfu.cheng@kuleuven.be

[2]School of Energy and Power Engineering, Jiangsu University,
Xuefu Road No. 301, Jingkou District, Zhenjiang, China, 212013
Phone: +86 18518979100
Email: yannan.wang@ujs.edu.cn

[3]Department of Chemical Engineering, Izmir Institute of Technology
Urla Izmir, Turkey,
Phone: + +90 2327506617
Email: abhishekdutta@iyte.edu.tr

Keywords: CFD, multiphase flow, mixing, AOD

## INTRODUCTION

The argon-oxygen decarburization (AOD) process is a crucial refining method in modern stainless steel production. It has been widely used to remove C in the past few decades [1, 2]. The AOD converter can provide excellent mixing conditions through turbulent stirring using submerged tuyeres. In the AOD process, the flow characteristics in the bath have a significant influence on the mass transport, momentum exchange and heat transfer, which are closely linked with the gas-metal reaction kinetics and the refining efficiency. A deep understanding of jet behavior, bubble flow characteristics and mixing efficiency facilitates further optimization of the decarburization and desulfurization operations. This will increase the AOD productivity and lower its energy and material consumption as well as the manufacturing cost [1].

The Computational Fluid Dynamics (CFD) technique has been proven effective in solving the complex flow field in AOD converters, and a series of CFD-based models have been developed. Tilliander *et al.* [3] developed a 3D single tuyere AOD model, in which a separate AOD tuyere model verified by Laser Doppler Anemometer (LDA) measurements [4, 5] was used to describe the pressure inlet boundary conditions. In their later work [6], this model was extended to simulate a six tuyeres AOD converter, and the fluid slag phase was also included. The model successfully predicted the fluid flow, turbulence, bubble behavior and liquid steel-slag dispersion. Wei *et al.* carried out a sequence of studies on the combined side and top blowing AOD process through numerical simulations [7, 8]. The influence of the tuyere angle, side-tuyere number and gas flow rate on the fluid characteristics and mixing efficiency were reported. The tuyere number and the tuyere angle had little effect on the overall mixing characteristics but certainly caused local variations in the mixing efficiency[1, 2]. Their work also showed that the top lance did not change the essential features of mixing created by the side blowing but significantly increased the turbulent kinetic energy and changed the local flow pattern.

Although previous studies have given significant insights into the multiphase flow phenomena in the AOD process, many phenomena such as multi-jets penetration, multi-bubble columns merging, and mixing characteristics still need to be investigated due to the process complexity. This study aims to reproduce the mixing characteristics in a 6-tuyere AOD process. A 3D multiphase flow model was developed based on the Eulerian multiphase flow approach. The drag force, as well as lift, virtual, turbulent dispersion and wall lubrication forces, are incorporated in the model.

 

## MODELLING

The present study focuses on the gas-liquid flow in the AOD process, and the following assumptions are adopted:

1. The initial temperature of liquid steel is set at 1873 K.
2. The physical parameters (*i.e.,* density, viscosity and thermal conductivity) of liquid steel are constant.
3. The liquid steel is incompressible, while the gas phase is considered to be compressible; thus, the transport equations of enthalpies of gas will be solved.

The simulation is based on the three-dimensional Eulerian multiphase flow approach. The momentum interfacial interaction between the gas and liquid phase was modeled by the interphase force, which is given by:

$$F_{lg} = -F_{gl} = F_D + F_L + F_{VM} + F_{TD} + F_{WL} \tag{1}$$

where $F_{lg}$ ($F_{gl}$) represents the momentum transfer from the liquid (gas) phase to the gas (liquid) phase, and the terms of $F_D$, $F_L$, $F_{VM}$, $F_{TD}$ and $F_{WL}$ on the right-hand side represent the drag force, lift force, virtual mass force, turbulent dispersion force and wall lubrication force, respectively.

The turbulence simulation was performed with the renormalization group (RNG) $k$-$\varepsilon$ model [9], where the transport equations of turbulent kinetic energy and its dissipation rate were solved. The RNG model provides an analytical formula for turbulent Prandtl numbers and uses an additional term in the $\varepsilon$ equation to improve the accuracy of rapidly strained and swirling flows; therefore, it is more accurate and reliable for a broader class of flows than the standard $k$-$\varepsilon$ model.

The ideal gas law was employed to calculate the density of the injected gas for every time step. Energy equations were enabled to calculate the heat transfer process. The ideal gas law is:

$$\rho_g = \frac{P_{op} + P}{\frac{R}{M_w}T} \tag{2}$$

where $P_{op}$ represents the operating pressure, $P$ is the local relative pressure, $R$ is the universal gas constant, $M_w$ is the molecular weight of the gas, and $T$ is the static temperature in K. The Sutherland viscosity law [10], which resulted from a kinetic theory based on an idealized intermolecular-force potential, was employed to account for the temperature-dependent viscosity.

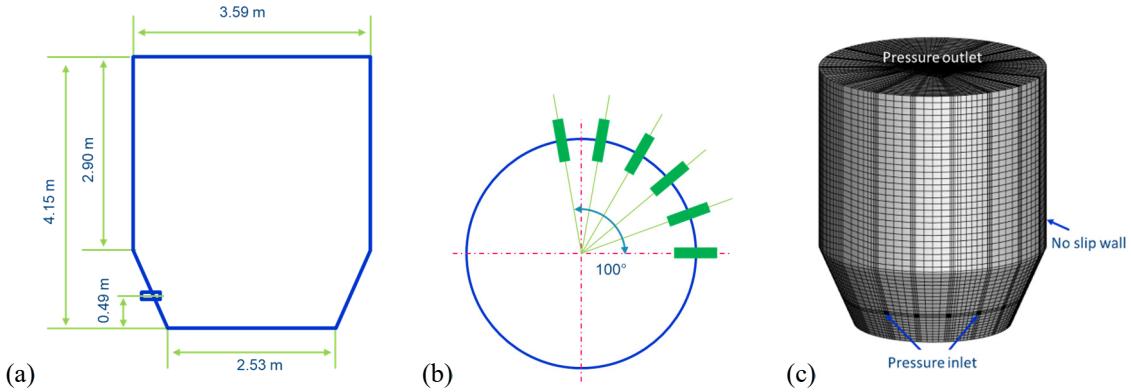


Figure 1. Schematic diagram of (a) geometry of the 6-tuyere AOD reactor, (b) tuyere configuration, and (c) generated grid.

A full three-dimensional model of a 120 t AOD reactor was developed. The geometry of the AOD is shown in Figure 1, and the six tuyeres were equiangular distributed in the range of 100 degrees (Figure 1 (b)). The calculation domain consists of a gas zone and a steel zone. Structured meshes with various numbers of cells were built by using ICEM. We used three meshes for mesh independence validation, and the mesh numbers are 271 462, 507 006 and 740 250, respectively. The results indicate that when the mesh number exceeds 507 006, only a tiny difference in the average vertical and horizontal steel velocity in the various horizontal planes (within 5%) can be found with the other meshes. Therefore, the mesh with the cell number 507 006 is sufficient for the current 3D simulation. No-slip wall boundary conditions were applied to the surrounding surfaces and bottom wall. The tuyere injection was set as the pressure inlet using various pressures for the modeling cases, and the top surface was used as an open boundary. The solution scheme of phase-coupled SIMPLE was used to solve the governing equations. Second-order upwind is applied for the momentum discretization terms. The time step size starts from $1\times10^{-5}$ s. Such a case runs until the solution is reasonably converged, and then the time step is appropriately scaled. After obtaining a stable flow field, the mixing time was calculated by injecting the tracer based on the species transfer model. The mixing time was defined as the time interval from the addition of the tracer until its concentration reached within 5% of the equilibrium value

 

## DISCUSSION

### 1. Penetration Depth

Figure 2 shows the multi-jets distribution along the axial direction of the tuyere from the tuyere tip to the jet-plane center for the six-tuyere AOD reactor. The side jets (labeled jets 1 and 6) penetrate more profound than the inner jets (labeled jets 2 to 5), leading to a larger gas fraction of the side jets at the same axial distance. That is because all gas jets are directed to the center of the jet plane and significantly influence each other. The side jets are squeezed less than the inner jets, thereby generating deeper penetration.

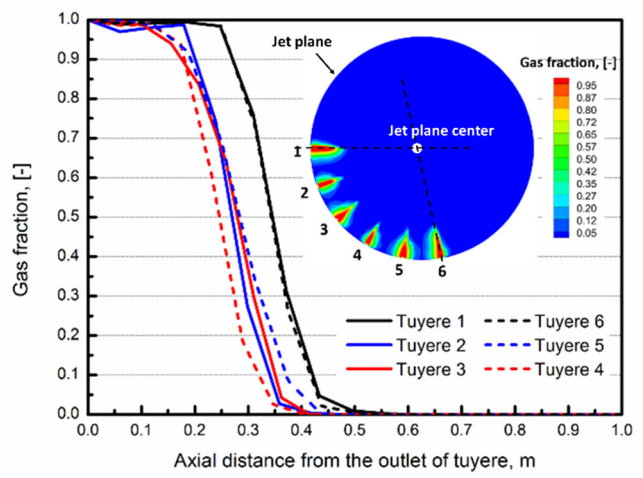


Figure 2. Multi-jets distribution along the axial direction of the tuyere for the six-tuyere AOD with an inlet pressure of 0.6 Mpa.

### 2. Flow Distribution

Figure 3 shows the distribution of the liquid steel velocity and the streamlines in the 6-tuyere AOD reactor. A first high liquid steel velocity zone is formed in the gas jet and bubble plume zones due to the momentum transfer from the gas phase to the liquid phase. The wide bubble plume with a high rising height indicates a strong ability to lift the molten steel. Another high-velocity zone is then generated in the upper part of the reactor due to the impact of the falling liquid steel on the molten bath (Figure 3 (a)), which could cause loss of stirring energy. The rising bubble plume cluster (the combined 6 bubble plumes) drives the liquid steel to form a clockwise main circulation in the AOD bath as shown in Figure 3 (b). Such a flow pattern could accelerate the mixing of the liquid bath.

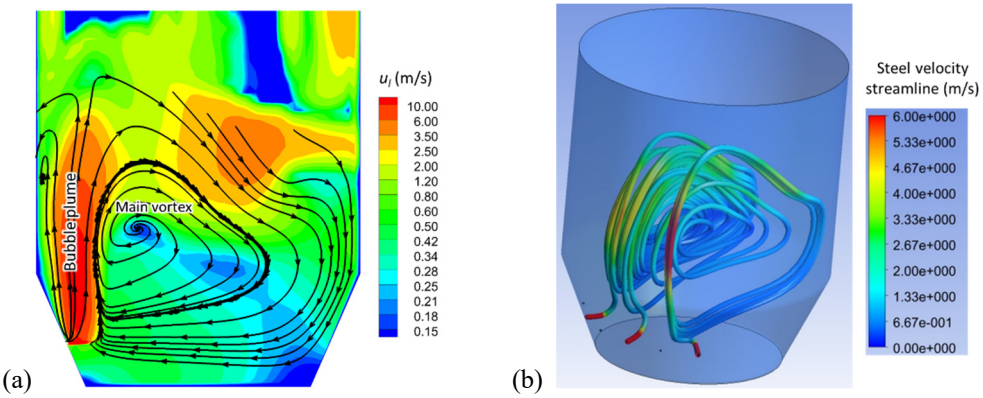


(a) (b)

Figure 3. The distribution of (a) liquid steel velocity and (b) streamline distribution in the 6-tuyere AOD reactor with an inlet pressure of 0.6 Mpa.

### 3. Mixing Characteristics

The tracer was added from the left side of the tuyeres (see Figure 4, $t$ = 0 s). Figure 4 shows the tracer concentration variations from 0 to 80 seconds in the 6-tuyere AOD reactor with an inlet pressure of 0.6 MPa. In the initial stage (*e.g.,* $t$ = 5 s), the rising bubble plumes drive the tracer upwards along the reactor wall, forming a high tracer concentration region near the left side of the tuyeres. The main circulation blocks the transverse flow of the tracer but accelerates the mixing perpendicular to the view direction; therefore, the tracer concentration is low near the wall opposite the tracer addition point, and the distribution follows vertical zones. The tracer flows across the main circulation in the upper bath, causing the right-side tracer concentration to increase from top to bottom (*i.e.,* $t$ = 10 s). A slow mixing zone (*i.e.,* flow dead zone) is present near the bottom corner of the wall opposite the tuyeres, where the tracer concentration remains relatively low until $t$ = 40 s.

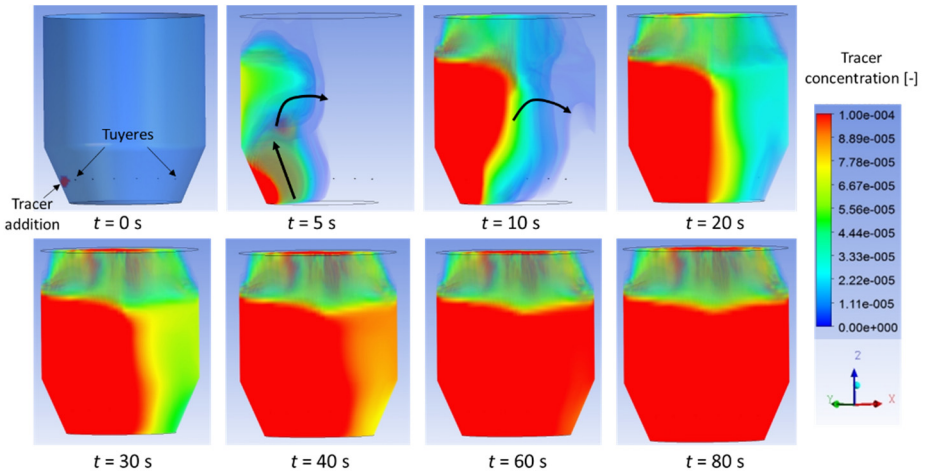


Figure 4. Tracer distribution from 0 to 80 s in the 6-tuyere AOD reactor with an inlet pressure of 0.6 Mpa.

Figure 5 shows the influence of the total gas flow rate on the mixing time in the 6-tuyere AOD reactor. The mixing time decreases firstly with increasing gas flow rate, minimizing at a gas flow rate of 2.59 kg/s, and then increases with increasing gas flow rate. This is because the increase of the gas flow rate increases the stirring energy, accelerating the bath mixing, while a further increase of gas flow rate could lead to the transition of flow regime from the bubbly flow to heterogeneous flow, thereby decelerating the bath mixing. The optimized gas flow rate is about 2.59 kg/s for the current AOD reactor. Although the model did not directly consider the metallurgical reactions, it provides the flow and mixing characteristics. These findings can be further extended to investigate the gas-metal reactions in the AOD reactor.

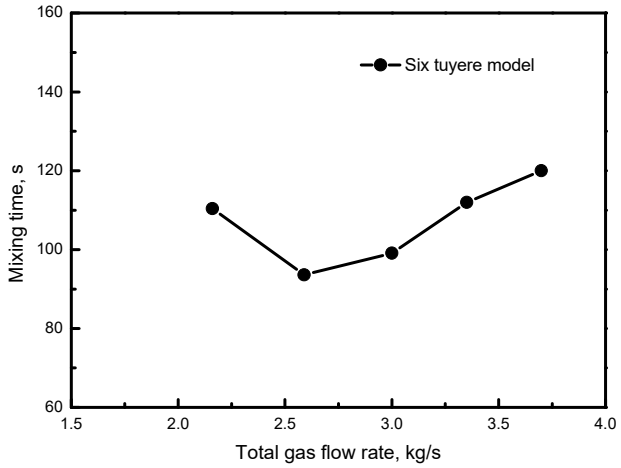


Figure 5. The influence of total gas flow rate on the mixing time in the 6-tuyere AOD.

 

## CONCLUSIONS

The flow behavior and mixing characteristics in a 6-tuyere AOD reactor were simulated by a 3D CFD model based on the Eulerian multiphase flow approach. The following conclusions were obtained:

1. The gas jets of the multi-tuyere system significantly influence each other. The side jets penetrate more profound than the inside jets.
2. A clockwise main circulation is in the bath center of the AOD reactor and dominates the bath mixing.
3. The flow dead zone *(i.e.,* zone with low mixing efficiency) is near the bottom corner of the wall opposite the tuyeres.
4. The mixing time firstly decreases with increasing flow rate and then increases. The optimized gas flow rate of the present AOD process is 2.59 kg/s.

## REFERENCES


1. J. Wei, H. Zhu, H. Chi, and H. Wang, "Physical modeling study on combined side and top blowing AOD refining process of stainless steel: gas stirring and fluid flow characteristics in bath," *ISIJ International*, Vol. 50, No. 1, 2010, pp. 17-25.
2. J. Wei, H. Zhu, H. Chi, and H. Wang, "Physical modeling study on combined side and top blowing AOD refining process of stainless steel: Fluid Mixing Characteristics in Bath," *ISIJ International*, Vol. 50, No. 1, 2010, pp. 26-34.
3. A. Tilliander, T. L. I. Jonsson, and P. G. Jönsson, "Fundamental mathematical modeling of gas injection in AOD converters," ISIJ International, Vol. 44, No. 2, 2004, pp. 326-333.
4. A. Tilliander, T. L. I. Jonsson, and P. G. Jönsson, "A mathematical model of the heat transfer and fluid flow in AOD nozzles and its use to study the conditions at the gas/steel interface," *ISIJ International*, Vol. 41, No. 10, 2001, pp. 1156-1164.
5. A. Tilliander, P. G. Jönsson, T. L. I. Jonsson, and S. Lille, "An experimental and numerical study of fluid flow in AOD Nozzles," Iron & steelmaker, Vol. 29, No. 2, 2002, pp. 51-57.
6. A. Tilliander, T. L. I. Jonsson, and P. G. Jönsson, "A three-dimensional three-phase model of gas injection in AOD converters," *steel research international*, Vol. 85, No. 3, 2014, pp. 376-387.
7. J. Wei, Y. He and G. Shi, "Mathematical modeling of fluid flow in bath during combined side and top blowing AOD refining process of stainless steel: application of the model and results," *steel research international*, Vol. 82, No. 6, 2011, pp. 693-702.
8. J. Wei, Y. He and G. Shi, "Mathematical modeling of fluid flow in bath during combined side and top blowing AOD refining process of stainless steel: mathematical model of the fluid flow," *steel research international*, Vol. 82, No. 6, 2011, pp. 703-709.
9. V. Yakhot and S. A. Orszag, "Renormalization group analysis of turbulence. I. Basic theory," *Journal of scientific computing*, Vol. 1, No. 1, 1986, pp. 3-51.
10. F.M. White: Viscous Fluid Flow (3d ed.), McGraw-Hill, New York (2005).


 